inorganics

MDPI

Article

The Impact of Arginine Side Chains on the Mechanism of Polycondensation of Silicic Acid in Bioinspired Mineralization

Jose Lanuza [1,2,3] and Enrico Ravera [1,2,3,*]

[1] Department of Chemistry "Ugo Schiff", Università degli Studi di Firenze, Via della Lastruccia 3, 50019 Sesto Fiorentino, Italy; josemanuel.lanuzadelgado@unifi.it
[2] Magnetic Resonance Center (CERM), Università degli Studi di Firenze, Via Luigi Sacconi 6, 50019 Sesto Fiorentino, Italy
[3] Consorzio Interuniversitario Risonanze Magnetiche di Metalloproteine (CIRMMP), Via Luigi Sacconi 6, 50019 Sesto Fiorentino, Italy
* Correspondence: ravera@cerm.unifi.it or enrico.ravera@unifi.it

Abstract: The polycondensation of silica from soluble silicic acid is at the basis of several chemical processes. The usual industrial route requires harsh pH conditions and high concentrations of the precursor molecules, not to mention a thermal treatment for obtaining condensed structures. On the other hand, biological organisms can promote the precipitation of silica under physiological conditions, including temperature and pH, and low concentrations of precursors. The key to this process is the use of polycationic molecules. Despite the relevance of these processes in modern industrial inorganic chemistry, this fascinating process is still not completely understood. Recent studies converge in pointing out that the role of the polycation is to create supersaturation of silicic acid in its immediate proximity, which would explain the impact of the polycation on the reaction rates. However, it remains unclear whether these polycations also directly influence the reaction mechanism at a molecular level. In this manuscript, we address this question by analyzing the reaction pathway of silicic acid dimerization in the presence of guanidinium as a mimic of the arginine side chain, through DFT calculations. We found that the impact on the reaction pathway is minimal, which strengthens the hypothesis of the local supersaturation driven by the polycationic molecules.

Keywords: bioinspired silica; lysozyme–silica composite; silicification reaction mechanism

check for updates

Academic Editors: Claudio Pettinari, Maurizio Peruzzini and Iolinda Aiello

Received: 22 April 2025
Revised: 12 June 2025
Accepted: 17 June 2025
Published: 19 June 2025

Citation: Lanuza, J.; Ravera, E. The Impact of Arginine Side Chains on the Mechanism of Polycondensation of Silicic Acid in Bioinspired Mineralization. *Inorganics* **2025**, *13*, 206. https://doi.org/10.3390/inorganics13060206

Copyright: © 2025 by the authors. Licensee MDPI, Basel, Switzerland. This article is an open access article distributed under the terms and conditions of the Creative Commons Attribution (CC BY) license (https://creativecommons.org/licenses/by/4.0/).

1. Introduction

Silicon(IV) dioxide (silica) is one of the most abundant materials in the contemporary chemical industry, because of its abundance and unique thermal and mechanical properties. The global silica market was valued at approximately USD 49–56 billion in recent years and is forecast to nearly double—reaching over USD 100 billion by 2030—with compound annual growth rates in the range of 9.9–10.2% [1]. The main types of silica used in industry are high-purity quartz, vitreous silica, fumed silica, silica gel, and diatomaceous earth (kieselguhr) [2]. The latter—the principal uses of which are in filtration plants, but also abrasives, fillers, insulating materials, and in the manufacturing of pozzolan—is a naturally occurring sedimentary rock formed over millions of years from the remains of diatoms. These unicellular algae (diameters in the 0.01–0.1 mm range) [3] have the property of accreting silica on their cell walls [4–8], which preserves the shape of the organism after death. This astonishing property of diatoms appears to be intimately linked to the use of polycationic molecules [9–11]. Over the years, the function of these polycationic molecules

has been studied in greater and greater detail [12–18]. One hypothesis brought about by Lenoci and Camp [19,20] is that the polycations facilitate silicification by forming an environment in which silicic acid can be concentrated through coacervation—or liquid–liquid phase separation. This hypothesis has gained considerable experimental support, obtained by Kurzbach and Becker at the University of Vienna [21,22] and Gal at the Weizmann Institute of Science [23,24].

Based on the role of polycations in the deposition of silica [25], Coradin, Coupé, and Livage in 2003 [26], and Luckarift, Dickerson, Sandhage, and Spain in 2006 proposed that lysozyme—a small polycationic protein could cause the deposition of silica [27]. However, the behavior of lysozyme presents a seemingly contradictory case, as it does not undergo coacervation under typical silicification conditions [28–30]. This apparent discrepancy can be reconciled by considering the colloidal nature of proteins [31], where the inherent positive charge density of lysozyme acts similarly to a pre-existing phase separation, effectively concentrating silicic acid around its surface. In this light, the results from molecular simulations indicating that silicic acid tends to cluster around positively charged patches on the lysozyme surface [32] are perfectly coherent with the results obtained from polyamines and silicification peptides described above. Other computational evidence has been obtained [33], indicating the role of hydrogen bonding residues. One aspect that remains unresolved is whether specific charged functional groups also alter the reaction profile of silica condensation, or if the catalytic effect is only related to a local supersaturation of the soluble precursors. Preliminary results from our previous work seem to suggest that the reaction mechanism is not altered by the presence of the arginine side chain [32], at least if the anion attack mechanism (AAM) is supposed to take place [34].

In this work, we use Density Functional Theory (DFT) methods [34] to investigate this mechanism (AAM) and the molecular attack mechanism (MAM) [33]. The reaction mechanisms are calculated in the presence and in the absence of guanidinium ions and of explicit water intervening water molecules to emulate and elucidate the effect of arginine in this condensation reaction.

2. Results

For the sake of clarity, we present the computational results in two separate sections, one for each of the two possible reaction mechanisms identified in [34]: the molecular attack mechanism (MAM) and the anion attack mechanism (AAM). The difference between mechanisms is the protonation state of the nucleophile during the attack. In the MAM, the silicic acid remains neutral during its approach to the silicon atom of the second silicic acid molecule; however, in the AAM, a prior proton transfer occurs before the attack, enhancing the nucleophilic character of the attacking molecule. Both mechanisms seem plausible under different circumstances, i.e., in systems in which the proton transfer is favored due to the stronger basicity of the present species, a faster attack of the resulting anionic species should follow. On the contrary, if the system is able to stabilize the neutral species near the electrophile through hydrogen bonds, a concerted mechanism could be quicker.

For both mechanisms, we test the effect of the presence of a guanidinium ion, which mimics the side chain of arginine residues. This choice is motivated by the experimental observation of a mononuclear tetrahedral species interacting with the R14 side chain of lysozyme in the presence of titanium(IV) bis-ammonium lactate [28]. For silicon(IV), under the same conditions, no crystal structure could be obtained. In that case, the interaction between the side chain and the tetrahedral species occurs via two intervening water molecules. For this reason, we tested both the presence of the guanidinium ion only and that of guanidinium and the two water molecules [32]. Since we studied the effect of guanidinium and water molecules on the reaction mechanism, we also performed

the calculations needed for a prior evaluation of the non-affected mechanism with the same methodology. As a methodological note, we neglect two possibilities because of the experimental conditions we are concerned with. We do not consider the possibility that the arginine side chain can be deprotonated, which would significantly impact the reaction mechanism as previously demonstrated [35]. However, under the experimental conditions that we are considering (pH around neutrality), the molar fraction of the deprotonated side chain is of the order of 10^{-5} or below. We do not consider the presence of anions in the vicinity of the side chain, because in the high-dielectric environment of water, the association between anions and cations is not particularly strong. In any case, in the following, we show that even water molecules reduce the impact of guanidinium, which implies that an intervening anion would have an even larger effect.

2.1. Molecular Attack Mechanism

In the MAM, the silicic acid acts as a nucleophile in its molecular form (i.e., as a neutral species). We assumed that the positive charge of the guanidinium ion causes the closer silicic acid molecule to act as the acceptor. The possible transition states (as such, with guanidinium, and with both guanidinium and intervening water molecules) are shown in Figure 1, whereas the corresponding energetics are given in Table 1. The "Products" state refers to the first local minimum after the transition state, and therefore may represent an unstable intermediate. This is the case in most product states, where it is apparent that the leaving water molecule is still within bonding distance of the silicon atom. An exception is shown in Figure 2, panel c, where the leaving water has already dissociated and indeed has a lower energy value than the product. This study focuses on the initial dimerization step of silicic acid polycondensation. This simplification allows us to isolate and examine the direct influence of the guanidinium group on the fundamental reaction mechanism (MAM vs. AAM) and the transition state energetics. While subsequent steps are undoubtedly important in the overall process of silica formation, the dimerization step is considered the rate-determining step and is crucial for understanding the initiation of polymerization. It is acknowledged that this approach does not capture the complexities of longer-range interactions or the influence of the growing silica network, which will be addressed in future work.

Table 1. Energetic and geometric data for the molecular attack mechanism (MAM) of silicic acid dimerization. R, TS, and P denote reactant, transition state, and product, respectively. G represents the presence of guanidinium, GW indicates the presence of guanidinium and two water molecules, and GW+ indicates the presence of guanidinium and a shell of 10 water molecules. Relative energies (ΔE_{elec}, ΔH, and ΔG) are given in kcal/mol, Si-O(LG) refers to the bond distance between silicon and the leaving group oxygen, Si-O(Nu) refers to the bond distance between silicon and the nucleophile oxygen, and O-H distances are given in Å.

Species	**ΔE_{elec}**	**ΔH**	**ΔG**	**Si-O(Nu)**	**O(LG)-H**	**O(Nu)-H**
Unit	**kcal/mol**	**kcal/mol**	**kcal/mol**	**Å**	**Å**	**Å**
R	0.00	0.00	0.00	3.584	0.990	1.756
TS	22.62	20.38	22.00	1.932	1.490	1.046
P	19.49	19.72	19.84	1.805	1.866	0.984
R-G	0.00	0.00	0.00	3.476	1.005	1.645
TS-G	19.37	17.45	19.86	1.886	1.534	1.034
P-G	17.37	17.87	18.98	1.796	1.908	0.982
R-GW	0.00	0.00	0.00	3.428	1.005	1.628
TS-GW	16.31	14.23	16.47	1.853	1.563	1.027
P-GW	14.70	15.00	16.07	1.785	1.873	0.984
R-GW+	0.00	0.00	0.00	3.302	1.006	1.607
TS-GW+	15.56	14.52	17.19	1.850	1.757	1.002
P-GW+	11.91	12.27	13.67	1.758	2.351	1.065

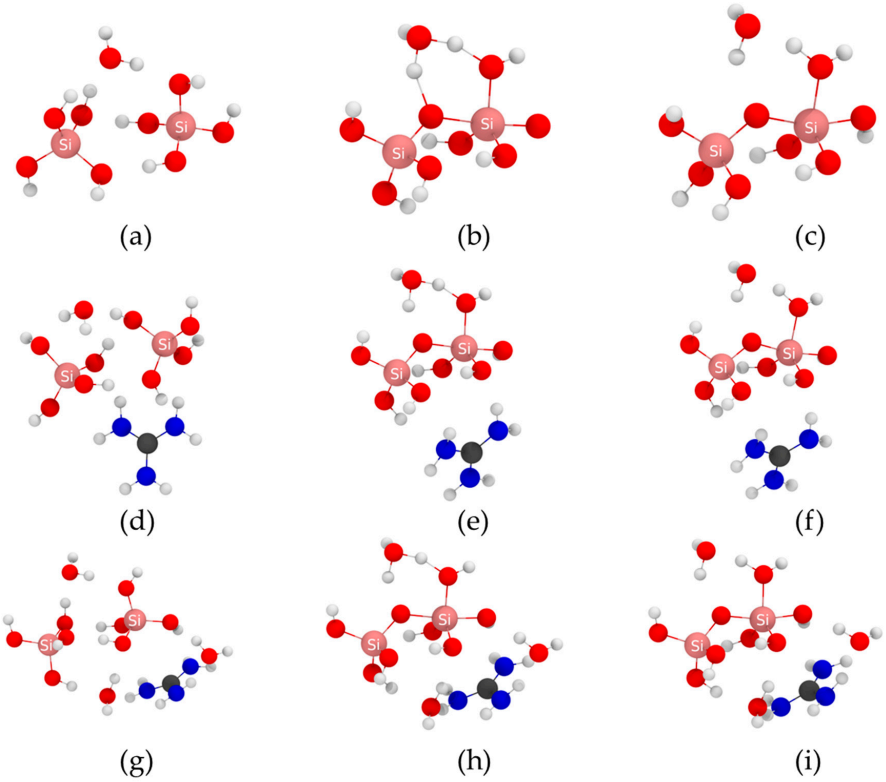


Figure 1. Reactant (**left**), transition (**center**), and product (**right**) states for the MAM: (**a**–**c**) in absence of guanidinium, (**d**–**f**) in presence the guanidinium (G), and (**g**–**i**) in presence of guanidinium and two extra water molecules (GW). Color code for atoms is: H—white, C—black, N—blue, O—red, and Si—pink.

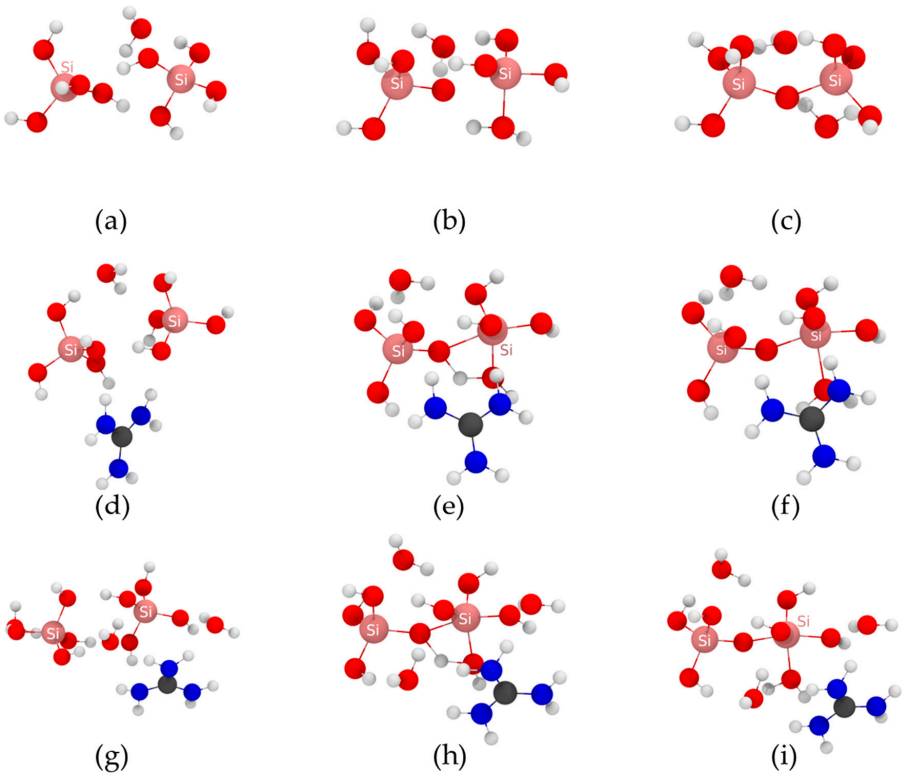


Figure 2. Reactant (**left**), transition (**center**), and product (**right**) states for the AAM: (**a**–**c**) in absence of guanidinium, (**d**–**f**) in presence the guanidinium (G), and (**g**–**i**) in presence of guanidinium and two extra water molecules (GW). Color code for atoms is: H—white, C—black, N—blue, O—red, and Si—pink.

2.2. Anion Attack Mechanism

In the AAM, silicic acid acts as a nucleophile in its singly deprotonated form (a monoanion). Given that the pKa for the first dissociation of silicic acid is approximately 9, only about 10% of silicic acid molecules are deprotonated at pH 8. This suggests that while the AAM is feasible, its contribution to the overall reaction rate under the relevant experimental conditions may be limited compared to the MAM. However, in microenvironments with locally elevated pH values, the AAM could become more significant. Also in this case, we assumed that the positive charge of the guanidinium ion would cause the closer silicic acid molecule to act as the acceptor. The possible transition states (as such, with guanidinium, and with both guanidinium and intervening water molecules) are shown in Figure 2, whereas the corresponding energetics are given in Table 2.

Table 2. Energetic and geometric data for the anion attack mechanism (AAM) of silicic acid dimerization. Labels are the same as in Table 1.

Species	ΔE_{elec}	ΔH	ΔG	Si-O(Nu)	O(LG)-H	O(Nu)-H
Unit	**kcal/mol**	**kcal/mol**	**kcal/mol**	**Å**	**Å**	**Å**
R	0.00	0.00	0.00	3.572	0.993	1.698
TS	28.48	27.87	29.85	2.204	1.565	1.021
P	2.30	1.92	1.83	1.669	2.883	0.973
R-G	0.00	0.00	0.00	3.761	0.975	3.274
TS-G	27.33	24.78	26.49	1.967	1.260	1.162
P-G	17.25	17.83	17.90	1.726	2.315	0.974
R-GW	0.00	0.00	0.00	4.589	0.983	1.769
TS-GW	25.36	23.26	25.23	1.929	1.239	1.183
P-GW	16.31	17.19	20.25	1.727	2.142	0.976
R-GW+	0.00	0.00	0.00	3.521	0.989	1.683
TS-GW+	27.51	24.84	25.38	1.931	1.233	1.184
P-GW+	−1.29	−1.75	−1.93	1.666	1.828	0.979

3. Discussion

The computational results obtained from the reaction mechanism calculations for both the MAM and the AAM provide a deeper insight into the role of the guanidinium side chain of arginine in the initial phases of silicic acid polycondensation to silica. In the case of MAM, the presence of guanidinium leads to a noticeable decrease in the activation free energy barrier, lowering it from 22.00 kcal/mol (unassisted) to 19.86 kcal/mol (guanidinium only) and 16.47 kcal/mol (guanidinium with water). Although the present results indicate that guanidinium can facilitate the process, the reaction mechanism does not appear to change dramatically. The transition states remain qualitatively similar, and the geometric changes induced are consistent with increased hydrogen bonding and electrostatic stabilization rather than any fundamental mechanistic alteration. The AAM pathway, has higher intrinsic activation energy (29.85 kcal/mol) (with respect to the models used in [34,35] we found that MAM has a lower barrier and the difference is to be attributed to the introduction of an additional water molecule in the model, which stabilizes differently the transitions states), but also shows a reduced activation energy in the presence of guanidinium (25.23 kcal/mol), which is in agreement with the hypothesis of guanidinium stabilizing the transition state through electrostatic interactions. In both cases, the observed reduction in activation energy by guanidinium is consistent with electrostatic stabilization of the transition state, and the inclusion of explicit intervening water molecules leads to a decrease in the activation energy with respect to only guanidinium. Increasing the number of water molecules does not have a major impact on the results of the calculations, implying that the most relevant interactions were already considered (GW+ rows in Tables 1 and 2). It is important to acknowledge the limitations of this model: representing the arginine sidechain with a single

guanidinium ion simplifies the complex interactions at the protein surface, including side chain dynamics, and the presence of other amino acid residues; furthermore, focusing solely on the dimerization step neglects the potential influence of the growing silica oligomers on the reaction pathway. Despite these simplifications, our results provide insights into the early-stage interactions between arginine and silicic acid leading to polycondensation: these results support our previous suggestion that positively charged groups such as arginine primarily act by increasing the local concentration of reactants via electrostatic attraction, thus promoting polycondensation through local supersaturation. The catalytic role of arginine is secondary and does not result from a substantial mechanistic transformation but rather from a modest transition state stabilization due to electrostatic and steric effects. This is also in line with the observations on coacervates by the groups of Gal, Kurzbach, and Becker, where the polycations act as scaffolds, bringing reactants together and creating an environment conducive to condensation.

4. Materials and Methods

All calculations were performed using the ORCA 5.0.1 package [36,37]. Density Functional Theory (DFT) was employed using the B3LYP functional [38–41] with the D3 general dispersion correction [42]. The computational methodology was selected based on previous computational results on the same reaction we investigated [34,35], and using the hybrid B3LYP functional over the GGA functionals BLYP or PBE because it has a better performance on structure optimization and single-point energy calculations for main group elements. The split-valence functional def2-SV(P) was selected, which includes polarization on non-hydrogen atoms [43]. For modeling the solvent, the conductor-like polarizable continuum model was used [44], albeit additional explicit solvent molecules were included in some calculations to cover relevant specific interactions.

The potential energy surface (PES) was explored in search of key stationary points related to reactant and product states (minima), as well as for the transition states (saddle points) for the different mechanisms. For that, the intrinsic reaction coordinates that connect the TSs with other key states were scanned thoroughly. The stationary points obtained were confirmed by frequency calculations that resulted in all vibrational modes positive for minima and one imaginary mode for saddle points on the PES [45]. The calculation of thermodynamic quantities was performed under standard conditions (298.15 K, 1 atm).

5. Conclusions

This study provides a detailed mechanistic evaluation of the role of guanidinium—a mimic of the arginine side chain—on the polycondensation of silicic acid, using DFT to model both the molecular and anion attack mechanisms. Our results show that while guanidinium does lower the activation barriers in both pathways, particularly in the MAM, its presence does not fundamentally change the overall reaction profile or mechanism. The main contribution appears to be through modest transition state stabilization and local structuring of the reaction environment rather than a direct catalytic effect.

These findings reinforce the hypothesis that polycationic species in bioinspired silica formation act primarily by creating localized supersaturation zones, facilitating proximity-induced condensation, rather than by altering the chemical pathway itself. Future studies may extend this analysis to include full protein environments or multivalent guanidinium clusters to further dissect the fine balance between electrostatics, solvation, and molecular orientation in biomimetic silica polymerization.

Author Contributions: Conceptualization, J.L. and E.R.; methodology, J.L.; formal analysis, J.L.; writing, J.L. and E.R.; project administration, E.R.; funding acquisition, E.R. All authors have read and agreed to the published version of the manuscript.

Funding: The financial support provided by the MUR—Dipartimenti di Eccellenza 2023–2027 (DICUS 2.0) to the Department of Chemistry 'Ugo Schiff' of the University of Florence is acknowledged. The authors acknowledge financial support under the National Recovery and Resilience Plan (NRRP), Mission 4, Component 2, Investment 1.1, Call for Tender No. 1409 published on 14 September 2022 by the Italian Ministry of University and Research (MUR), funded by the European Union NextGenerationEU project titled 'Mechanism of Bioinspired Inorganic Oxide Formation' (P2022JSC5Z, MInO), CUP D53D23016850001, Grant Assignment Decree No. 1386 adopted on 01/09/2023 by the MUR, and from the project 'Potentiating the Italian Capacity for Structural Biology Services in Instruct-ERIC' (ITACA.SB; Project No. IR0000009, CUP B53C22001790006) funded by the European Union NextGenerationEU under MUR call 3264/2021 PNRR M4/C2/L3.1.1.

Institutional Review Board Statement: Not applicable.

Informed Consent Statement: Not applicable.

Data Availability Statement: The inputs for the calculations are available in Zenodo with https://doi.org/10.5281/zenodo.15650388.

Acknowledgments: We acknowledge ISCRA for awarding this project access to the LEONARDO supercomputer, owned by the EuroHPC Joint Undertaking, hosted by CINECA (Italy).

Conflicts of Interest: The authors declare no conflicts of interest.

References

1. Global Silica Market Size, Share, Growth Analysis Report 2030. Available online: https://www.grandviewresearch.com/industry-analysis/silica-market (accessed on 10 March 2025).
2. Greenwood, N.N.; Earnshaw, A. *Chemistry of the Elements*; Elsevier: Amsterdam, The Netherlands, 2012; ISBN 978-0-08-050109-3.
3. Armbrust, E.V. The Life of Diatoms in the World's Oceans. *Nature* **2009**, *459*, 185–192. [CrossRef] [PubMed]
4. Sumper, M.; Kröger, N. Silica Formation in Diatoms: The Function of Long-Chain Polyamines and Silaffins. *J. Mater. Chem.* **2004**, *14*, 2059–2065. [CrossRef]
5. Sumper, M.; Brunner, E. Silica Biomineralisation in Diatoms: The Model Organism Thalassiosira Pseudonana. *ChemBioChem* **2008**, *9*, 1187–1194. [CrossRef] [PubMed]
6. Kröger, N.; Poulsen, N. Diatoms—From Cell Wall Biogenesis to Nanotechnology. *Annu. Rev. Genet.* **2008**, *42*, 83–107. [CrossRef]
7. Hildebrand, M.; Lerch, S.J.L.; Shrestha, R.P. Understanding Diatom Cell Wall Silicification—Moving Forward. *Front. Mar. Sci.* **2018**, *5*, 125. [CrossRef]
8. Mayzel, B.; Aram, L.; Varsano, N.; Wolf, S.G.; Gal, A. Structural Evidence for Extracellular Silica Formation by Diatoms. *Nat. Commun.* **2021**, *12*, 4639. [CrossRef]
9. Hildebrand, M.; Volcani, B.E.; Gassmann, W.; Schroeder, J.I. A Gene Family of Silicon Transporters. *Nature* **1997**, *385*, 688–689. [CrossRef]
10. Kröger, N.; Deutzmann, R.; Sumper, M. Polycationic Peptides from Diatom Biosilica That Direct Silica Nanosphere Formation. *Science* **1999**, *286*, 1129–1132. [CrossRef]
11. Kröger, N.; Deutzmann, R.; Bergsdorf, C.; Sumper, M. Species-Specific Polyamines from Diatoms Control Silica Morphology. *Proc. Natl. Acad. Sci. USA* **2000**, *97*, 14133–14138. [CrossRef]
12. Poulsen, N.; Sumper, M.; Kröger, N. Biosilica Formation in Diatoms: Characterization of Native Silaffin-2 and Its Role in Silica Morphogenesis. *Proc. Natl. Acad. Sci. USA* **2003**, *100*, 12075–12080. [CrossRef]
13. Sumper, M. Biomimetic Patterning of Silica by Long-Chain Polyamines. *Angew. Chem. Int. Ed.* **2004**, *43*, 2251–2254. [CrossRef] [PubMed]
14. Lutz, K.; Gröger, C.; Sumper, M.; Brunner, E. Biomimetic Silica Formation: Analysis of the Phosphate-Induced Self-Assembly of Polyamines. *Phys. Chem. Chem. Phys.* **2005**, *7*, 2812–2815. [CrossRef] [PubMed]
15. Lechner, C.C.; Becker, C.F.W. Exploring the Effect of Native and Artificial Peptide Modifications on Silaffin Induced Silica Precipitation. *Chem. Sci.* **2012**, *3*, 3500–3504. [CrossRef]

16. Poulsen, N.; Scheffel, A.; Sheppard, V.C.; Chesley, P.M.; Kröger, N. Pentalysine Clusters Mediate Silica Targeting of Silaffins in Thalassiosira Pseudonana. *J. Biol. Chem.* **2013**, *288*, 20100–20109. [CrossRef]
17. Lechner, C.C.; Becker, C.F.W. A Sequence-Function Analysis of the Silica Precipitating Silaffin R5 Peptide. *J. Pept. Sci.* **2014**, *20*, 152–158. [CrossRef]
18. Lechner, C.C.; Becker, C.F.W. Silaffins in Silica Biomineralization and Biomimetic Silica Precipitation. *Mar. Drugs* **2015**, *13*, 5297–5333. [CrossRef]
19. Lenoci, L.; Camp, P.J. Self-Assembly of Peptide Scaffolds in Biosilica Formation: Computer Simulations of a Coarse-Grained Model. *J. Am. Chem. Soc.* **2006**, *128*, 10111–10117. [CrossRef]
20. Lenoci, L.; Camp, P.J. Diatom Structures Templated by Phase-Separated Fluids. *Langmuir* **2008**, *24*, 217–223. [CrossRef] [PubMed]
21. Strobl, J.; Kozak, F.; Kamalov, M.; Reichinger, D.; Kurzbach, D.; Becker, C.F. Understanding Self-Assembly of Silica-Precipitating Peptides to Control Silica Particle Morphology. *Adv. Mater.* **2023**, *35*, 2207586. [CrossRef]
22. Kozak, F.; Brandis, D.; Pötzl, C.; Epasto, L.M.; Reichinger, D.; Obrist, D.; Peterlik, H.; Polyansky, A.; Zagrovic, B.; Daus, F.; et al. An Atomistic View on the Mechanism of Diatom Peptide-Guided Biomimetic Silica Formation. *Adv. Sci.* **2024**, *11*, 2401239. [CrossRef]
23. Zhai, H.; Bendikov, T.; Gal, A. Phase Separation of Oppositely Charged Polymers Regulates Bioinspired Silicification. *Angew. Chem. Int. Ed. Engl.* **2022**, *61*, e202115930. [CrossRef]
24. Zhai, H.; Fan, Y.; Zhang, W.; Varsano, N.; Gal, A. Polymer-Rich Dense Phase Can Concentrate Metastable Silica Precursors and Regulate Their Mineralization. *ACS Biomater. Sci. Eng.* **2023**, *9*, 601–607. [CrossRef]
25. Coradin, T.; Durupthy, O.; Livage, J. Interactions of Amino-Containing Peptides with Sodium Silicate and Colloidal Silica: A Biomimetic Approach of Silicification. *Langmuir* **2002**, *18*, 2331–2336. [CrossRef]
26. Coradin, T.; Coupé, A.; Livage, J. Interactions of Bovine Serum Albumin and Lysozyme with Sodium Silicate Solutions. *Colloids Surf. B Biointerfaces* **2003**, *29*, 189–196. [CrossRef]
27. Luckarift, H.R.; Dickerson, M.B.; Sandhage, K.H.; Spain, J.C. Rapid, Room-Temperature Synthesis of Antibacterial Bionanocomposites of Lysozyme with Amorphous Silica or Titania. *Small* **2006**, *2*, 640–643. [CrossRef]
28. Gigli, L.; Ravera, E.; Calderone, V.; Luchinat, C. On the Mechanism of Bioinspired Formation of Inorganic Oxides: Structural Evidence of the Electrostatic Nature of the Interaction between a Mononuclear Inorganic Precursor and Lysozyme. *Biomolecules* **2021**, *11*, 43. [CrossRef]
29. Pyne, P.; Mitra, R.K. Excipients Do Regulate Phase Separation in Lysozyme and Thus Also Its Hydration. *J. Phys. Chem. Lett.* **2022**, *13*, 931–938. [CrossRef]
30. Bruno, F.; Gigli, L.; Ferraro, G.; Cavallo, A.; Michaelis, V.K.; Goobes, G.; Fratini, E.; Ravera, E. Lysozyme Is Sterically Trapped Within the Silica Cage in Bioinspired Silica–Lysozyme Composites: A Multi-Technique Understanding of Elusive Protein–Material Interactions. *Langmuir* **2022**, *38*, 8030–8037. [CrossRef]
31. Loeb, J. The colloidal behavior of proteins. *J. Gen. Physiol.* **1921**, *3*, 557–564. [CrossRef] [PubMed]
32. Macchiagodena, M.; Fragai, M.; Gallo, A.; Pagliai, M.; Ravera, E. The Role of Lysozyme in the Formation of Bioinspired Silicon Dioxide. *Chem. A Eur. J.* **2024**, *30*, e202401249. [CrossRef] [PubMed]
33. Novi Inverardi, G.; Petrolli, L.; Carnovale, F.; Bartocci, A.; Taioli, S.; Lattanzi, G. Adsorption of Silica Oligomers on Biomolecules: Structural and Dynamical Insights for Atom Probe Tomography via Classic Molecular Dynamics Simulations. *Comput. Struct. Biotechnol. J.* **2025**, *27*, 2537–2543. [CrossRef]
34. Liu, X.; Liu, C.; Meng, C. Oligomerization of Silicic Acids in Neutral Aqueous Solution: A First-Principles Investigation. *Int. J. Mol. Sci.* **2019**, *20*, 3037. [CrossRef]
35. Liu, X.; Liu, C.; Feng, Z.; Meng, C. The Promoter Role of Amines in the Condensation of Silicic Acid: A First-Principles Investigation. *ACS Omega* **2021**, *6*, 22811–22819. [CrossRef]
36. Neese, F.; Wennmohs, F.; Becker, U.; Riplinger, C. The ORCA Quantum Chemistry Program Package. *J. Chem. Phys.* **2020**, *152*, 224108. [CrossRef]
37. Neese, F. Software Update: The ORCA Program System—Version 5.0. *WIREs Comput. Mol. Sci.* **2022**, *12*, e1606. [CrossRef]
38. Becke, A.D. A New Mixing of Hartree–Fock and Local Density-functional Theories. *J. Chem. Phys.* **1993**, *98*, 1372–1377. [CrossRef]
39. Lee, C.; Yang, W.; Parr, R.G. Development of the Colle-Salvetti Correlation-Energy Formula into a Functional of Electron Density. *Phys. Rev. B* **1988**, *37*, 785–789. [CrossRef]
40. Vosko, S.H.; Wilk, L.; Nusair, M. Accurate Spin-Dependent Electron Liquid Correlation Energies for Local Spin Density Calculations: A Critical Analysis. *Can. J. Phys.* **1980**, *58*, 1200–1211. [CrossRef]
41. Stephens, P.J.; Devlin, F.J.; Chabalowski, C.F.; Frisch, M.J. Ab Initio Calculation of Vibrational Absorption and Circular Dichroism Spectra Using Density Functional Force Fields. *J. Phys. Chem.* **1994**, *98*, 11623–11627. [CrossRef]
42. Grimme, S.; Antony, J.; Ehrlich, S.; Krieg, H. A Consistent and Accurate Ab Initio Parametrization of Density Functional Dispersion Correction (DFT-D) for the 94 Elements H-Pu. *J. Chem. Phys.* **2010**, *132*, 154104. [CrossRef]
43. Weigend, F.; Ahlrichs, R. Balanced Basis Sets of Split Valence, Triple Zeta Valence and Quadruple Zeta Valence Quality for H to Rn: Design and Assessment of Accuracy. *Phys. Chem. Chem. Phys.* **2005**, *7*, 3297–3305. [CrossRef]

44. Barone, V.; Cossi, M. Quantum Calculation of Molecular Energies and Energy Gradients in Solution by a Conductor Solvent Model. *J. Phys. Chem. A* **1998**, *102*, 1995–2001. [CrossRef]
45. Fukui, K. The Path of Chemical Reactions—The IRC Approach. *Acc. Chem. Res.* **1981**, *14*, 363–368. [CrossRef]

Disclaimer/Publisher's Note: The statements, opinions and data contained in all publications are solely those of the individual author(s) and contributor(s) and not of MDPI and/or the editor(s). MDPI and/or the editor(s) disclaim responsibility for any injury to people or property resulting from any ideas, methods, instructions or products referred to in the content.